FOREDUNE CLASSIFICATION AND STORM RESPONSE: AUTOMATED ANALYSIS OF TERRESTRIAL LIDAR DEMS

KATHERINE L. BRODIE[1], NICHOLAS J. SPORE[1]

1. *U.S. Army Engineer Research and Development Center, Coastal & Hydraulics Laboratory, Coastal Observation & Analysis Branch, 1261 Duck Rd, Duck, NC 27949, USA. Katherine.L.Brodie@usace.army.mil; Nicholas.J.Spore@usace.army.mil*

Abstract: Accurate predictions of foredune response and recovery to storms are critical for understanding coastal vulnerability at a variety of time-scales. Foredune morphology and storm response were investigated using terrestrial lidar data along a 10-kilometer stretch of open-coast beach near Duck, NC. An algorithm was developed to classify foredune state from 50-cm bare earth DEMs into four categories: scarped, recovering, healthy, and man-made. The algorithm was based on extraction of morphological features including the slope, volume, and curvature of the foredune face. Preliminary results detailing the response of each foredune state to a 4-day Nor'Easter (Hs = 4.8m at 16s in 8m of water) are presented, and suggest that man-made and recovering dunes lost more volume and eroded more rapidly when compared with scarped dunes. The increased erosion may have been due to a combination of slightly lower dune-toe elevations for the man-made dunes and unconsolidated sediment in the foredune.

Introduction

Foredunes are a naturally-occurring coastal defense against extreme storm inundation and are an integral part of coastal systems, particularly on developed coastlines where they protect property and infrastructure from storm inundation. In natural systems, these features are built by wind-blown sand transported from the beach, and eroded during storms by large waves and surge, serving as a source of sediment to the littoral system (Aubrey 1979). On developed coastlines, human intervention can artificially speed recovery processes, through beach scraping and dune-building activities, altering the natural cycle (Nordstrom 2008). Accurate predictions of the response of foredunes to large storm events, and their subsequent re-growth, are therefore critical to evaluating the vulnerability of coastal communities. The landfall of Hurricane Sandy on the US northeast coast in 2013 highlighted the significance of coastal foredunes; areas without dunes experienced severe socioeconomic and physical destruction costing state and federal agencies millions of taxpayer dollars (USACE 2013). In the aftermath, resources have been devoted towards developing new approaches for assessing the vulnerability and resilience of U.S. coastlines, with particular emphasis on understanding and enhancing the benefits of nature-based infrastructure such as coastal foredunes.

Foredune morphology is often described in storm impact prediction models (e.g. Sallenger 2000) using the elevation of the dune crest and dune toe (D_{high} and D_{low} respectively) from airborne lidar data, which are compared with maximum runup elevations to categorize the expected storm impact and predicted responses (Stockdon et al. 2007). For example, when total water levels are above the dune toe, but below the dune crest, the impact regime is classified as "collision" and the expected morphology response is slumping or scarping of the dune face. Foredunes which have undergone recent wave attack in the collision regime therefore feature steep, near-vertical faces. Regions with foredunes with comparatively low D_{low} elevations experience more erosion during storms, and are therefore considered more vulnerable (Stockdon et al. 2007; Splinter et al. 2014). While the amount of dune retreat in the collision regime scales largely with the duration of wave attack to the dune face (Larson et al. 2004), characteristics of the dune other than its crest or toe elevation, such as alongshore variations in morphology (Houser 2013), vegetation coverage, pore space and infiltration rate (Palmsten and Holman 2011), or surface curvature (e.g. undercutting, (Erikson et al. 2007)), may also enhance or impede rates of morphologic change, and are not included in the simple storm impact models. For example, an old, well-vegetated and compacted dune may erode much more slowly during wave impact when compared with a recently pushed pile of sand with the same D_{high} and D_{low}.

In contrast to foredunes that have recently undergone erosion, recovering foredunes exhibit markedly different morphology—the foredune face generally exhibits a lower, more variable slope, with convex features indicating Aeolian deposition and active re-growth processes in the form of incipient foredune growth (Thom and Hall 1991). Plant density, wind speed & direction, sediment availability, frequency of runup inundation, and human intervention (both positive and negative) can affect rates of foredune recovery and overall morphology (Hesp 2002; Nordstrom 1994; Nordstrom and Jackson 2013).

Dune morphology is typically quantified using elevation point data, with the past decade seeing the rise of airborne lidar systems for coastal dune monitoring (e.g. Woolard & Colby 2002; Mitasova et al. 2005). The spatial resolution of most airborne lidar data is roughly 1 elevation point per square meter and is collected at near-nadir angles making observations of morphological details on the foredune face difficult. Terrestrial lidar data, however, is collected from a vehicle driven on the beach and can acquire 100s-1000s of data points per square meter, particularly on near vertical dune faces. These data enable a detailed characterization of subtle alongshore and cross-shore variations in foreshore topography, however, the data are often under-utilized because analysis and feature extraction can be time and personnel intensive.

The goal of this work is to develop automated approaches to extract detailed morphological features from terrestrial lidar data that may be used to classify the "state" of the foredune, as well as investigate any correlations between pre-storm dune state and dune response. Foredunes are classified into 4 states: scarped, recovering, healthy, and man-made based on unique morphologic features that are automatically extracted from terrestrial lidar data, and pre-, during, and post-storm terrestrial lidar surveys are used to observe alongshore variations in dune response to a 6-day nor'Easter along 10 kilometers of coastline on a sandy, open-coast beach near Duck, NC.

Field Site & Storm Conditions

The field site is located within a 12 kilometer stretch of open coast beach fronting the Atlantic Ocean in Duck, North Carolina, containing the U.S. Army Corps of Engineers Field Research Facility (FRF) pier and property (Figure 1A). This section of coast and its surroundings are comprised of a sandy seabed with grain sizes ranging from 0.53 mm to 8.0 mm and exposed to waves predominately from the northeast in the winter and spring months, and from the south-southeast in the summer and fall months.

During Hurricane Sandy in November 2012, most of the dunes within the study site were subject to prolonged periods of runup collision, with as much as 10 meters of dune retreat measured in the most impacted areas. In the aftermath of Hurricane Sandy, some homeowners utilized dump trucks or bull-dozers to rebuild dunes in front of their homes in preparation for the winter storm season, particularly within a 1.5 km region from ~8000m to 9500 m alongshore (Figure 1). This stretch of coastline has been experiencing increased erosion rates since the early 2000s, and will be the focus of this work due to the high variability in dune morphology within this region.

A nor'Easter impacted the study site beginning on March 6, 2013 (Figure 1B). Waves remained above 3 m in 8 m of water depth for 4 days, with the largest waves occurring on March 10, 2013 (Hs = 4.8 m at 16 s in 8 m of water depth). This storm marked the first significant dune collision event since Hurricane Sandy.
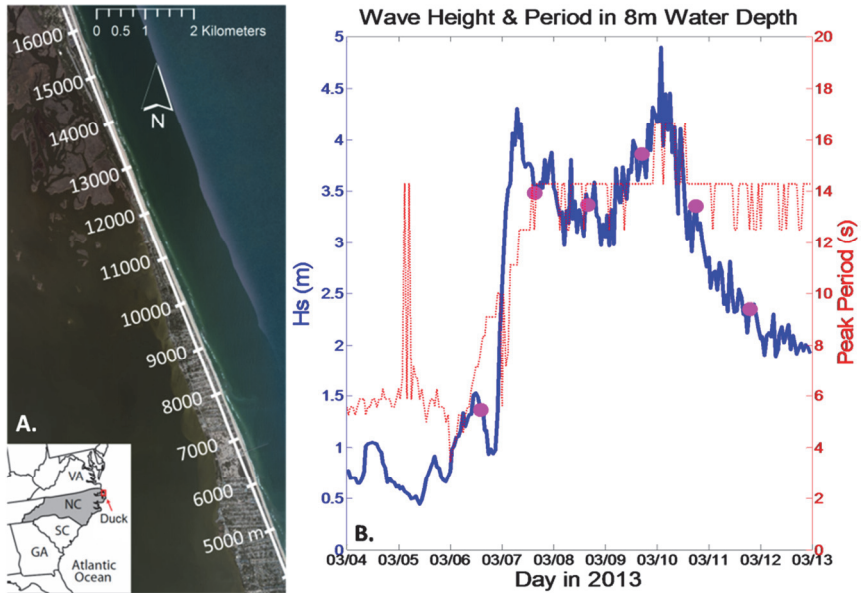
Figure 1. A. The study site in Duck, NC showing the alongshore coordinates of the local coordinate system. B. Significant wave height (blue) and peak wave period (red) during the storm, with survey times shown in magenta circles.

Methodology

Lidar Data collection

Mobile lidar surveys were conducted daily during the storm event (magenta circles, Figure 1B) using a Riegl VZ-1000 terriestrial laser scanner and a POS-LV 220 GNSS navigation system mounted on Coastal Lidar and Radar Imaging System (CLARIS). The VZ-1000 has a wavelength of 1550 nm (near-infrared) with a laser power of 300 kHz and scans at a fixed perpendicular angle to the direction of movement at approximately 60 lines/second. This creates a three-dimensional point cloud as the vehicle advances forward, illuminating 100-1000 points per square meter depending on vehicle speed and topography. The vehicle trajectory is measured by the POS-LV system which includes two GNSS GPS antennas and an L1/L2 GPS receiver, an inertial motion unit (IMU), and a distance measurement instrument (DMI) mounted to the wheel, to provide the best estimate of trajectory. The survey is completed in two alongshore passes: one driving north near the toe of the dune scanning down the profile to the shoreline and the other driving south near the shoreline scanning up the profile to the dune crest. This typically provides an area of overlap between the two passes that is used to assess the accuracy and integrity of the navigation data

throughout various spatial and temporal regions of the survey. After each survey, the scanner is boresighted to resolve any subtle angular differences between itself and the IMU due to environmental fluctuations that may lead to thermal expansion or contraction.

DEM Generation

Mobile lidar data are post-processed with multiple software packages to produce the final bare-earth digital elevation model. Terrestrial GPS data is post-processed with the National Geodetic Survey's Continuously Operating Reference Stations (CORS) in Duck, NC. The GPS data is combined with IMU and DMI data using a kalman filter within Applanix's POSPac GNSS software to derive a smoothed best estimate of trajectory (SBET) and QAQC metrics. The point cloud is then rectified in Riegl's RiProcess software using the SBET and boresight model. Survey accuracy is assessed through comparisons to known fixed features along the study site and is on the order of +/- 10cm. The point cloud is then post-processed using the terrain filter within RiProcess, and points are classified as water, vegetation, structures, and ground. The classified point cloud is exported as an .las file. The point cloud is rotated and translated into an alongshore/cross-shore local coordinate system fit to the linear trend of the shoreline (Figure 1A). A 50-cm bare-earth DEM is generated from the .las file by averaging point elevations within each grid cell. Bare-earth DEMs were generated for each survey for use in the subsequent analysis.

Dune Feature extraction

Morphologic features are extracted along each cross-shore transect every 50 cm along the coastline. The cross-shore curvature for each transect was also calculated to assist in defining morphologic features. The elevation of the dune toe (D_{low}) was found in a two step process (Figure 2), and was the most difficult parameter to extract robustly. The "first guess" D_{low} (red star, Figure 2) was found by finding the point on the cross-shore profile that was the farthest point from a linear fit (red line, Figure 2) between the position of the MHW contour (0.5 m NAVD88) and the maximum observed elevation on that profile (Mitasova et al., 2011). This location was then refined by selecting the point with the maximum positive curvature (green star, Figure 2) within +/- 10m in the cross-shore direction of the "first guess" (red dotted line, Figure 2). This second refinement was necessary because the true dune-crest is often not observed or easily identifiable from ground-based lidar due to the view of the scanner, making the linear fit between the dune crest and shoreline potentially unstable. To that end, the dune crest elevation (D_{high}) was defined as the point with the maximum peak in negative curvature (convex) landward of D_{low} or as the maximum observed elevation in that transect if no local minima in curvature

were observed. The average slope of the dune (β_{dune}) was defined as the slope of the best-fit linear trend in dune elevations between D_{low} and D_{high}. Foredune volume (V_{dune}) was similarly the integral under the points on the dune-face between D_{low} and D_{high}. The number of peaks in curvature (κ_{pks}) between D_{low} and D_{high} was used as a metric to describe the morphology and roughness of the foredune face. Future work will focus on developing algorithms that make use of the point cloud data in addition to the bare-earth DEM to incorporate vegetation coverage and the presence of sand-fencing and other constructive or destructive structures.
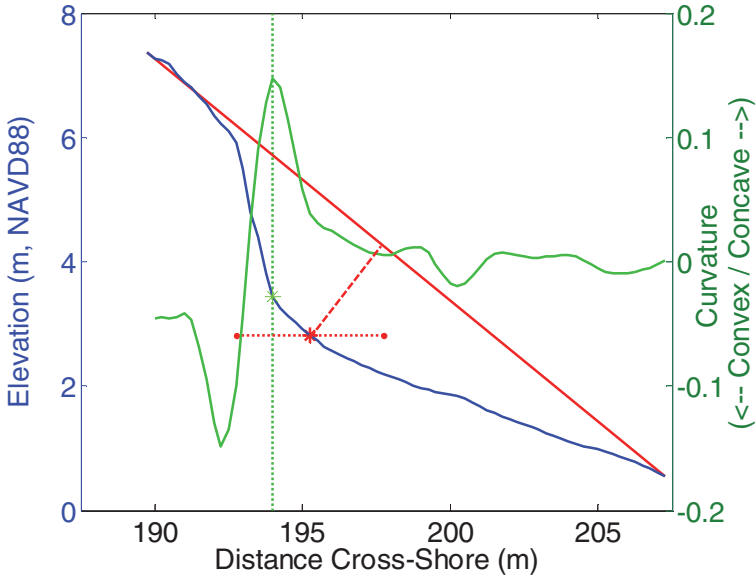
Figure 2 Dune-toe schematic showing elevation profile (blue), linear-fit (red line), first guess D_{low} (red star), dune-toe region (red-dotted line), curvature (green line), and final picked D_{low} (green star).

Dune Morphology

The morphology of the foredune face varied with location along the study site (Figure 3, left colors). The pre-storm dune morphology will be described in detail in the following paragraph. D_{low} was fairly constant at ~4 m in the northern section of coastline between 10000 and 16000 m alongshore. Between 9000 and 7500 m alongshore D_{low} was highly variable, oscillating between 2 and 4 m. South of the FRF pier (~7000m), D_{low} slowly increased from 4 to 5 m.

D_{high} averaged 6.6 m along the study site with a higher variance between 6000 and 12000 m alongshore. The lowest D_{high} elevations were found between 6000 and 9000 m alongshore. β_{dune} ranged between 0.2 and close to 1 (near vertical) with slopes >0.6 occurring primarily between 12000 and 16000 and between 7000 and 7500 (just north of the FRF pier). South of the FRF pier (<7000 m alongshore), and between 7500 and 12000 m alongshore slopes varied around 0.4, near the angle of repose for sand. Between 7500 and 9000 m, there were also some locations with steeper slopes (>0.6). V_{dune} was much lower (< 10 m^3/m) in the northern portion of the study site between of 12000 and 16000 m alongshore. South of 12000 m, V_{dune} was more variable, oscillating between < 10 and > 30 m^3/m. κ_{pks} ranged between 0 and 2 along the study site. Regions with κ_{pks} > 0 were found in a small region between 14000 and 15000 m alongshore, between 12000 and 9000 m alongshore, and south of the FRF pier (< 7000 m).

Dune-State Classification

Four distinct dune "states" were identified within the study-site region: scarped, recovering, healthy, and man-made. These states were identified because of their unique morphology and processes related to their formation. In addition, discussions with coastal engineers and managers suggested there was interest in being able to identify regions of the coastline that were recovering through natural Aeolian processes (more resilient) verses regions that were remaining in a scarped, more vulnerable state. This information would then enable focused mitigation efforts, such as sand fencing installation and plantings, in locations where it was needed most.

Example profiles for each dune-state and associated morphologic parameters are shown in Figure 4. Both recovering and healthy dunes (Figure 4A & B) were defined by having κ_{pks} >0, which was used to indicate active Aeolian processes (Thom and Hall 1991). On recovering dunes, incipient dune formation should occur at the base of the profile near the dune-toe (Hesp 2002) while the upper dune face will remain steeply scarped indicating recent wave-attack. In contrast, healthy dunes should have slopes closer to the angle of repose due to continual deposition and re-working by Aeolian processes, and have higher V_{dune} due to the long period of time since the last re-working by storm waves allowing for progradation of the foredune face. Therefore, of the dunes with κ_{pks} >0, dunes with steeper average slopes (β_{dune} >0.6) and lower volumes were classified as recovering, and the rest were classified as healthy.
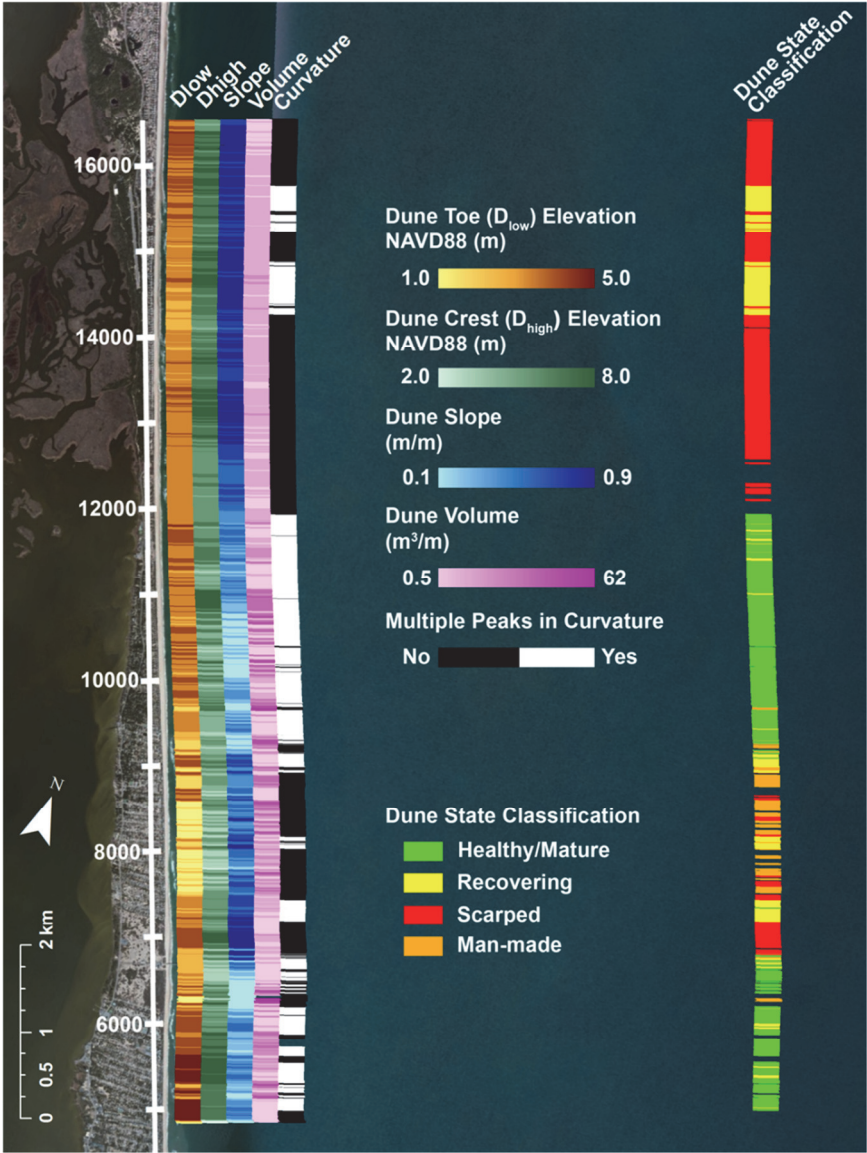
Figure 3 Dune morphology parameters (left) and classification (right).

Both scarped and manmade dunes (Figure 4C & D) are characterized by more linear foredune faces. Scarped dunes (Figure 4C) were defined as dunes with steep slopes (β_{dune} >0.6) and low dune volumes (V_{dune}< 12 m³/m), indicating

recent scarping by wave action with little to no recovery at the base of the foredune. In contrast, manmade dunes (Figure 4D) had slopes near the angle of repose (piles of unconsolidated sediment), larger volumes, and lower dune tow elevations.

Figure 4. Example profiles of each dune-state.

The pre-storm dune-state classification is shown by the red (scarped), orange (man-made), yellow (recovering), and green (healthy) colors along the right side of Figure 3. South of the FRF pier (< 7000 m alongshore), the foredune was classified as healthy, with some locations classified as recovering. This classification is in-line with qualitative assessments of the region, as the wide-beach allows for large fetches, enabling active Aeolian processes to occur. Between 7000 and 7500 m alongshore on the FRF property the dune is classified as scarped or recovering, consistent with a narrow, steep beach, and frequent impact by waves. Between 7500 and 9000 m alongshore, dune morphology is highly variable, including man-made, scarped, and some recovering dunes. This

is consistent with the erosional hotspot region described above that experienced significant erosion during Hurricane Sandy. The classification code correctly identified dunes that had been built by homeowners within this region as well as the dunes that were left in their more natural state (scarped or recovering). Some homeowners did erect sand-fencing following Hurricane Sandy, and this may be have lead to more rapid recovery and incipient dune formation in the 4 months post-Sandy leading to some dunes being classified as recovering. Between 9000 and 12000 m alongshore, there is a large stretch of mostly healthy, mature dunes, with a few regions of recovering dunes, consistent with a qualitative assessment of the area. This stretch of coastline also tends to have a wider, flatter beach, conducive for Aeolian transport. The remainder of the study site had scarped dunes, with the exception of two small regions which were recovering at 14500 and 15500 m alongshore. Interestingly, this region also features a relatively flat, wider, beach, so the marked transition from healthy, mature dunes to scarped dunes is poorly understood at this time. Alongshore variations in historical management techniques and offshore bathymetry will be investigated to identify any possible causes.

Future work will focus on using Bayesian Network techniques (e.g. Wikle and Berliner 2007) to improve quality of and uncertainty in dune-state classifications. In addition, we would like to test the classification code at a variety of field sites to determine robust thresholds and perhaps add additional dune-states.

Surf-zone Morphology and Wave Runup during the Storm

Surf-zone morphology was analyzed using time-average images of radar intensity also collected with CLARIS (e.g. Brodie and McNinch, 2011; not-shown). Time-average imagery shows waves were breaking over an outer storm bar during the 03-08 March surveys. In addition, an inner-sand bar was present south of the FRF pier (< 7000 m alongshore) and on the pier property through 7500 m alongshore. The inner sandbar appeared to weld with the shoreline between 7500 and 9000 m alongshore within the erosional hotspot region, and moved back offshore for the rest of the study site at 9000 m alongshore. Cross-shore sums in time-averaged radar intensity were therefore significantly lower between 7500 and 9000 m alongshore, potentially suggesting less dissipation of wave energy in this region (e.g. Brodie and McNinch, 2011). Wave runup was also calculated every 50 cm alongshore for the duration of the storm using Stockdon et al (2006) forced with the observed beach slope from the DEMs and observed wave parameters in 8-m of water depth (not shown). Predicted runup was found to exceed D_{low} for most of the region between 7500 and 9000 m alongshore during the 3 hours on either side of each of the 7 high tides from 08-11 March. This corresponded to the erosional hotspot region which featured

steep beach slopes, and also fewer offshore sandbars, as indicated above. Since hydrodynamic forcing was so different in this region compared to the rest of the study site, our analysis linking storm response with dune-state will be confined to within the erosional hotspot region.
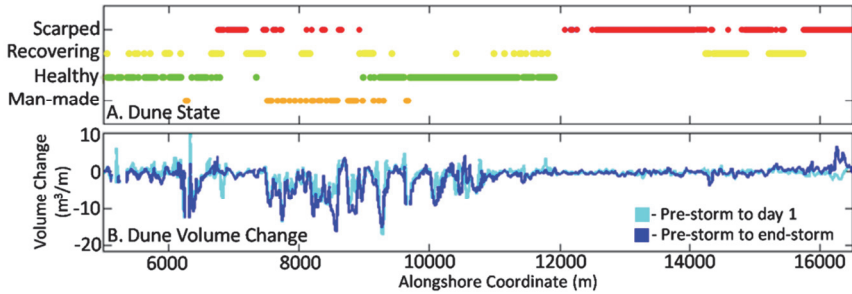

Figure 5. A. Dune state classification: man-made (red), healthy (yellow), recovering (green), and scarped (blue). B. Dune volume change in the first 24 hours (cyan) and for the whole storm (blue).

Storm Response

Dune volume changes from 06 to 07 March and 06 to 11 March are shown in Figure 5. The majority of dune volume change occurred between 7500 and 10000 m alongshore. The highest dune erosion rates occurred for man-made dunes within the erosional hotspot region (note relationship between locations with red markers in Figure 5A and largest negative peaks in Figure 5B). Daily dune profiles and calculated D_{low} retreat rates are shown for three example profiles in Figure 6: A. Recovering, B. Man-made, and C. Scarped. Initial beach slopes and D_{low} retreat slopes and rates are shown for each example profile. The man-made dunes had the highest retreat rates, averaging ~1 m/day, however, man-made dunes also tended to have lower D_{low} elevations. In addition, the recovering dunes eroded more rapidly when compared with the scarped dunes, perhaps owing to increased volumes of unconsolidated sediment (similar to the man-made dunes) at lower elevations associated with the formation of the incipient dune. The initial trajectory for D_{low} for the recovering and man-made dunes was down (from 06-07 March), whereas the scarped dune trajectory was up and backwards, similar to prior studies (Larson et al 2004; Palmsten and Holman 2012). After the initial erosion, however, the D_{low} trajectories were all directed upward and backward. The average slope of the D_{low} trajectories was similar to the initial beach slope for the man-made and scarped dunes, however, was roughly twice the beach slope for the recovering dune.

Future work will focus on testing the performance of dune erosion models (e.g. Palmsten and Holman 2011) to predict alongshore variations in dune-response

using these observations. We hypothesize the dune erosion models will perform better for the scarped dunes, since most were created based on data for slumping or scarping of consolidated dunes, but may not adequately characterize the erosion of unconsolidated man-made or recovering dunes as well.
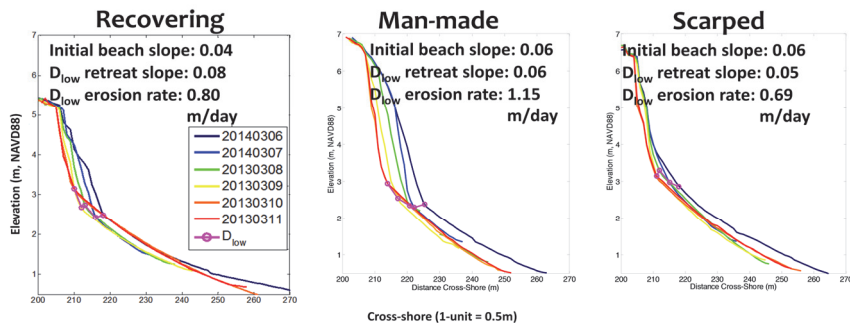

Figure 6. Example profiles during the storm.

Conclusions

An automated classification algorithm was developed to identify scarped, recovering, man-made, and healthy dunes from 50-cm bare-earth DEMs generated from terrestrial lidar data. Detailed terrestrial lidar data allowed subtle changes in curvature on the foredune face to be exploited and used to identify the presence of active Aeolian sediment transport. The slope and volume of the foredune face was also found to be indicative of foredune state, and used to discriminate recovering dunes from healthy dunes, and man-made dunes from scarped dunes. This classification scheme will allow coastal managers and engineers the ability to rapidly identify naturally resilient regions of the coast and determine where to focus mitigation efforts that enhance dune rebuilding processes.

In addition, the response of coastal foredunes along a 10-km region of open coast beach near Duck, NC was investigated using daily mobile terrestrial lidar scans during a 4-day Nor'Easter. Foredune response was analyzed in relation to pre-storm foredune state, and preliminary results suggest man-made and recovering dunes saw increased erosion of the foredune face compared to scarped dunes within a 1.5 km erosional hotspot. The man-made dunes had the highest rates of erosion (~1.15m/day), whereas the scarped dunes had the lowest rates of erosion (0.69 m/day). The increased erosion may have been due to a combination of unconsolidated sediment and slightly lower dune-toe elevations for the man-made dunes.

References

Erikson, L. H., Larson M., and Hanson, H.. (2007). "Laboratory Investigation of Beach Scarp and Dune Recession due to Notching and Subsequent Failure." *Marine Geology* 245 (1-4): 1–19. doi:10.1016/j.margeo.2007.04.006.

Hesp, P. (2002). "Foredunes and Blowouts: Initiation, Geomorphology and Dynamics." *Geomorphology* 48: 245–68. doi:10.1016/S0169-555X(02)00184-8.

Houser, C. (2013). "Alongshore Variation in the Morphology of Coastal Dunes: Implications for Storm Response." *Geomorphology* 199 (October): 48–61. doi:10.1016/j.geomorph.2012.10.035.

Larson, M., Erikson, L., and Hanson, H. (2004). "An Analytical Model to Predict Dune Erosion due to Wave Impact." *Coastal Engineering* 51 (8-9): 675–96. doi:10.1016/j.coastaleng.2004.07.003.

Mitasova, H., Hardin E., and Starek, M.J. (2011). "Landscape Dynamics from LiDAR Data Time Series." http://www.geomorphometry.org/system/files/Mitasova2011geomorphometry.pdf.

Mitasova, H., Overton M., and Harmon, R. S. (2005). "Geospatial Analysis of a Coastal Sand Dune Field Evolution: Jockey's Ridge, North Carolina." *Geomorphology* 72 (1-4): 204–21. doi:10.1016/j.geomorph.2005.06.001.

Nordstrom, K. F. (1994). "Beaches and Dunes of Human-Altered Coasts." *Progress in Physical Geography* 18: 497–516. doi:10.1177/030913339401800402.

Nordstrom, K. F. (2008). *Beach and Dune Restoration*. publisherNameCambridge University Press. http://dx.doi.org/10.1017/CBO9780511535925.

Nordstrom, K. F., and Jackson N. L. (2013). "Restoration of Coastal Dunes." In , edited by M. Luisa Martínez, Juan B. Gallego-Fernández, and Patrick A. Hesp. Springer Series on Environmental Management. Berlin, Heidelberg: Springer Berlin Heidelberg. doi:10.1007/978-3-642-33445-0.

Palmsten, M. L., and Holman, R. A. (2011). "Infiltration and Instability in Dune Erosion." *Journal of Geophysical Research* 116 (C10): C10030. doi:10.1029/2011JC007083.

Palmsten, M. L., and Holman, R.A. (2012). "Laboratory Investigation of Dune Erosion Using Stereo Video." *Coastal Engineering* 60 (February): 123–35. doi:10.1016/j.coastaleng.2011.09.003.

Sallenger Jr., A. H. (2000). "Storm Impact Scale for Barrier Islands." *Journal of Coastal Research* 16 (3). Coastal Education & Research Foundation, Inc.: 890–95. http://www.jstor.org/stable/4300099.

Stockdon, H. F., Holman, R. A., Howd, P. A., and Sallenger Jr, A. H. (2006). "Empirical Parameterization of Setup, Swash, and Runup." *Coastal Engineering* 53 (7): 573–88. http://www.sciencedirect.com/science/article/pii/S0378383906000044.

Stockdon, H. F., Sallenger Jr, A. H., Holman, R. A., and Howd, P. A. (2007). "A Simple Model for the Spatially-Variable Coastal Response to Hurricanes." *Marine Geology* 238 (1–4): 1–20. http://www.sciencedirect.com/science/article/pii/S0025322706003355.

Thom, B. G., and Hall, W. (1991). "Behaviour of Beach Profiles during Accretion and Erosion Dominated Periods." *Earth Surface Processes and Landforms* 16 (1991): 113–27. http://onlinelibrary.wiley.com/doi/10.1002/esp.3290160203/full.

USACE, (2013). "Hurricane Sandy Coastal Projects Performance Evaluation Study: Disaster Relief Appropriations Act, 2013." Report submitted to Congress by the Assistant Secretary of the Army for Civil Works, November 6, 2013. http://www.nan.usace.army.mil/About/Hurricane_Sandy/CoastalProjectsPerformanceEvaluationStudy.aspx

Wikle, C. K., and Berliner, L. M. (2007). "A Bayesian Tutorial for Data Assimilation." *Physica D: Nonlinear Phenomena* 230 (1-2): 1–16. doi:10.1016/j.physd.2006.09.017.

Woolard, J. W., and Colby, J. D. (2002). "Spatial Characterization, Resolution, and Volumetric Change of Coastal Dunes Using Airborne LIDAR: Cape Hatteras, North Carolina." *Geomorphology* 48 (1-3): 269–87. doi:10.1016/S0169-555X(02)00185-X.

Foredune Classification and Storm Response: Automated Analysis of Terrestrial Lidar DEMs

Kate Brodie & Nick Spore
ERDC-CHL-COAB

Coastal Sediments 2015 – San Diego, CA
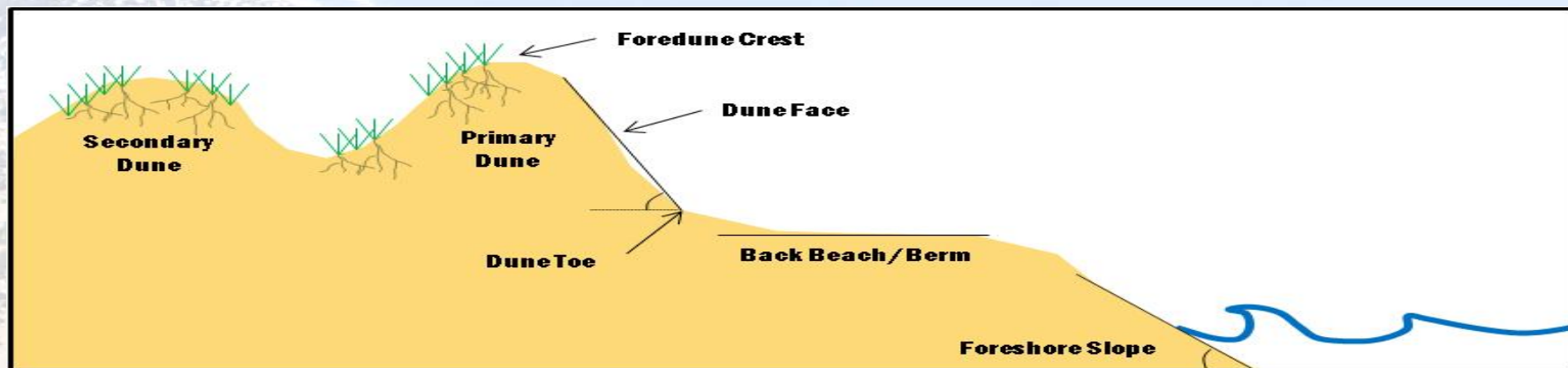**"Understanding and Working with Nature"**

Outline

1. What are we looking at?
2. Why do we care?
3. How was the data collected?
4. What to do with the data?
5. How is the analysis useful?
6. What can be improved upon?

Motivation

- Foredunes = Nature-based defensive infrastructure (especially along developed coastlines)

- Accurate storm-response and subsequent re-growth predictions → critical to assess resiliency and vulnerability

- Understanding and enhancing benefits of nature-based infrastructure post-Sandy (USACE)

- Classification = understand current state pre/post-storm and useful for decision makers

Motivation

Process Feedbacks

Coastline Dynamics
- erosion by waves
- geologic framework
- sediment supply
- storm magnitude/frequency
- beach/nearshore morphology
- barrier island response to sea level rise

erosion by waves

Aeolian Processes
- fetch-controlled sediment supply
- wind speed
- sediment size & type
- vegetation
- moisture content

vegetation deposition

Management
- anthropogenic sediment supply
- dune engineering
- planting vegetation
- sand fencing
- beach nourishment
- engineering structures

sand fencing

Foredune Form

Physical Features
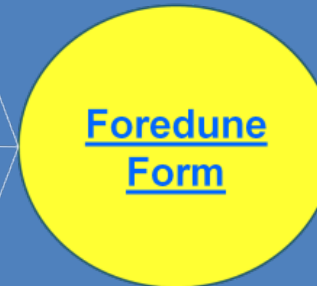
- Profile Slope
- Height
- Width
- Vegetation Density
- Curvature
- Alongshore Continuity

Motivation

- Storm-impact prediction models (e.g. Sallenger 2000, Stockdon et al. 2007) characterize dunes by:
  - Dune Toe
  - Dune Crest

- Other characteristics NOT included in models that may enhance/impede change include:
  - Alongshore variations in morphology (Houser 2013)
  - Vegetation coverage, pore space and infiltration rate (Palmsten and Holman 2011)
  - Surface curvature (Erikson et al. 2007)

- Airborne (1 point/sq m) vs. Terrestrial lidar (100s-1000s points/sq m)

- Dense datasets often underutilized

Methodology - Survey

- Mobile terrestrial lidar surveys performed daily along 11km stretch of coastline during 6-day Nor'easter
- Coupled with X-band radar to produce time-averaged images of radar intensity (i.e. wave breaking)
- Centered around low-tide for maximum foreshore exposure and personnel safety
- Largest waves on March 10: Hs = 4.8 m at 16 sec

Coastal Lidar and Radar Imaging System (CLARIS)

Wave Height & Period in 8m Water Depth

Day in 2013
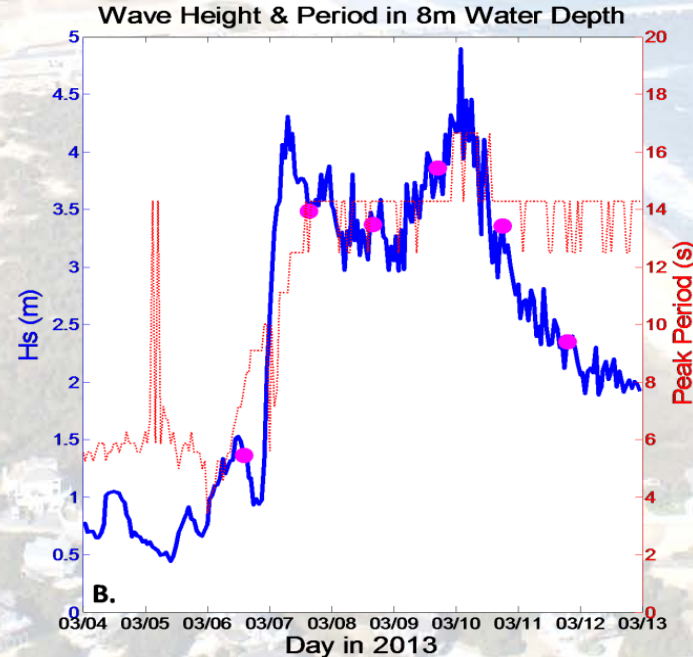
Nor'easter Storm Conditions

Study Site: Duck, NC

Methodology – Data Processing

Vegetation/Structures
Bare-Earth
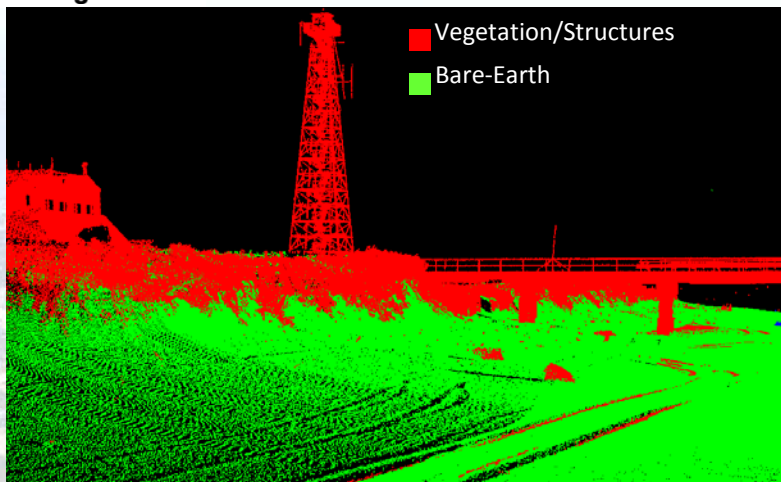
1. Point cloud rectification and filtering

2. Bare-earth DEM at 50 cm resolution

Elevation NAVD88 (m)

Alongshore Coordinate (m)

Cross-shore Coordinate (m)
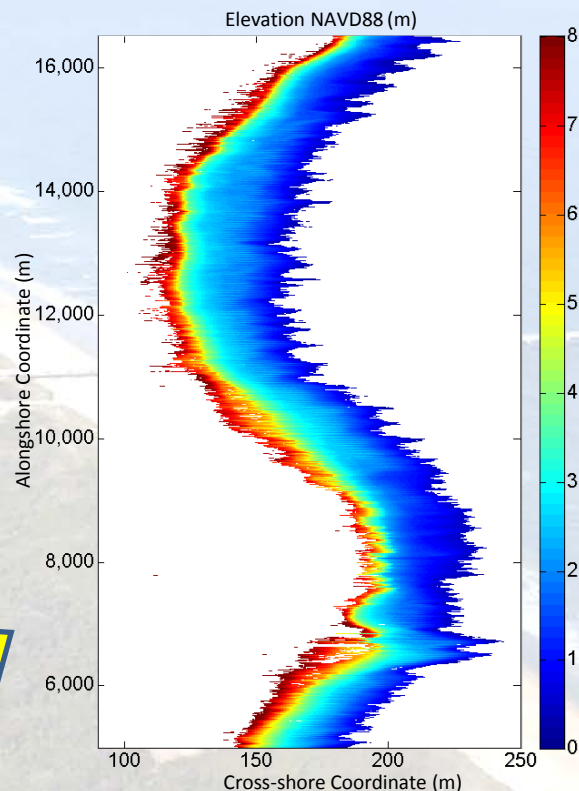
3. DEM rotated and translated into local alongshore/cross-shore coordinate system

4. Dune feature identification/ classification at every 0.5m transect

Dune Features

- Cross-shore Profile Curvature (κ_{pks})
- Dune Toe (D_{low}) Elevation
- Dune Crest (D_{high}) Elevation
- Dune Slope (β_{Dune})
- Dune Volume (V_{dune})
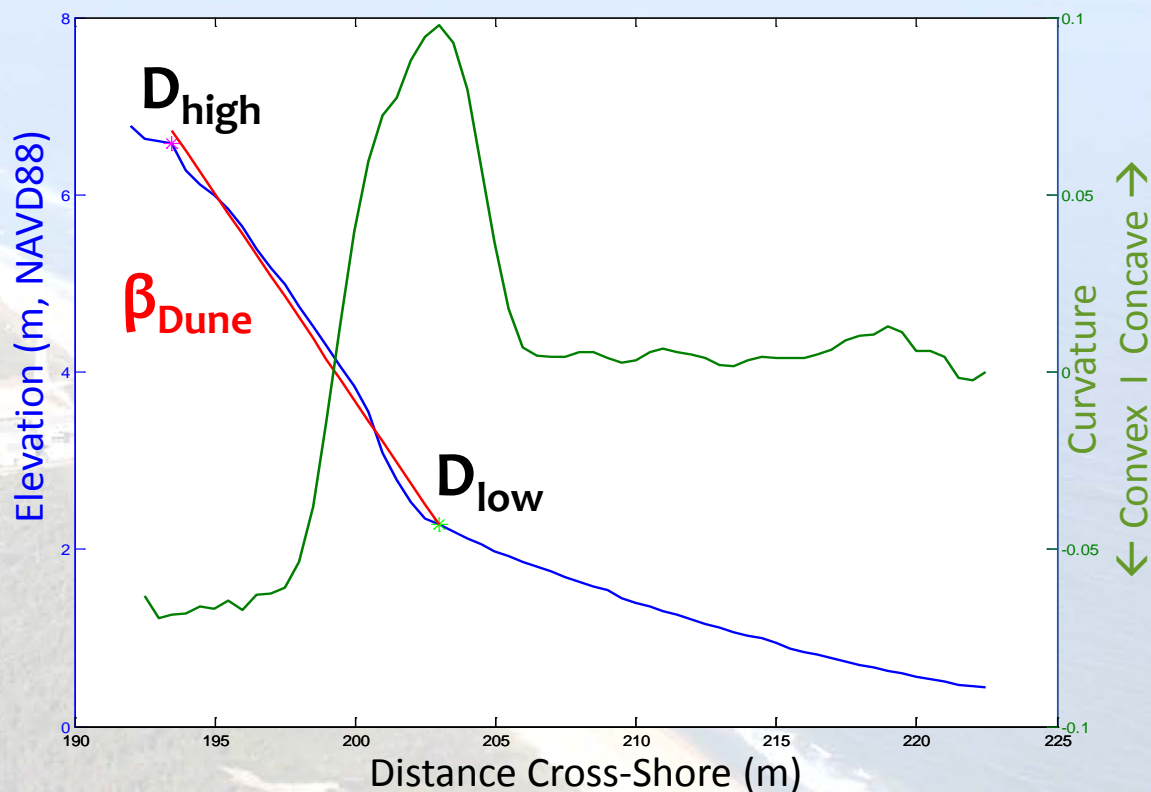
Feature Extraction

1. Fit "sheet"
2. D_{low} 1st guess
3. Refine guess
4. Define D_{high}
5. Fit β_{Dune}
6. Calc V_{dune}
7. Assess κ_{pks}
8. (Future...use point data for veg density/ structural presence)
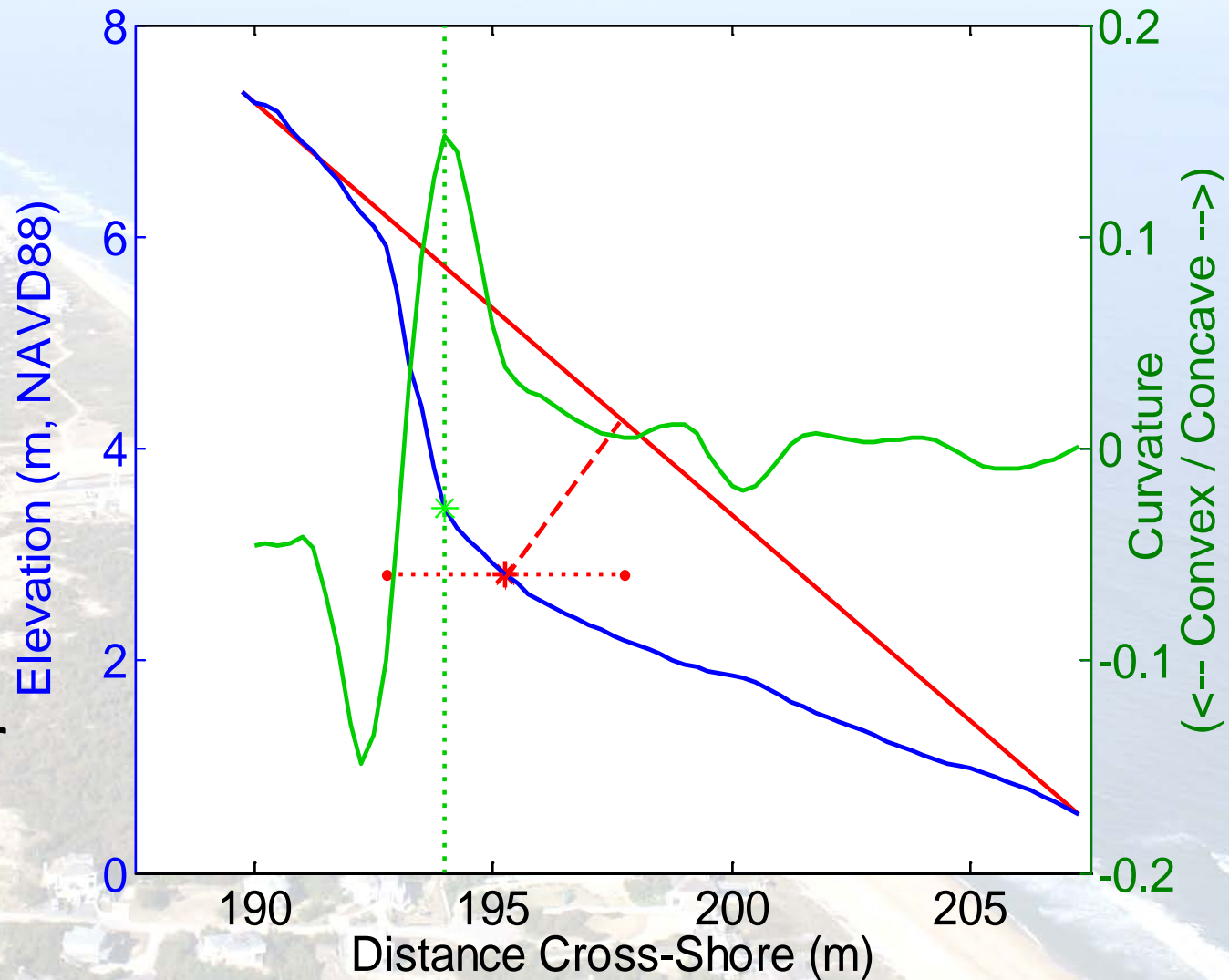
Classification

Four distinct "dune states" were identified within the study region based on:

– Morphologic uniqueness

– Process signatures related to their formation

– Recovering/resilient versus vulnerable

Dune States:

1. Recovering
2. Healthy/Mature
   Multiple Peaks in Curvature = YES

3. Scarped
4. Man-made
   Multiple Peaks in Curvature = NO

Classification

- Both recovering and healthy dunes are defined by $\kappa_{pks} > 0$ (i.e. multiple peaks in curvature)
- Indicative of active Aeolian processes (Thom and Hall, 1991)

Recovering
Profile at 8392m alongshore
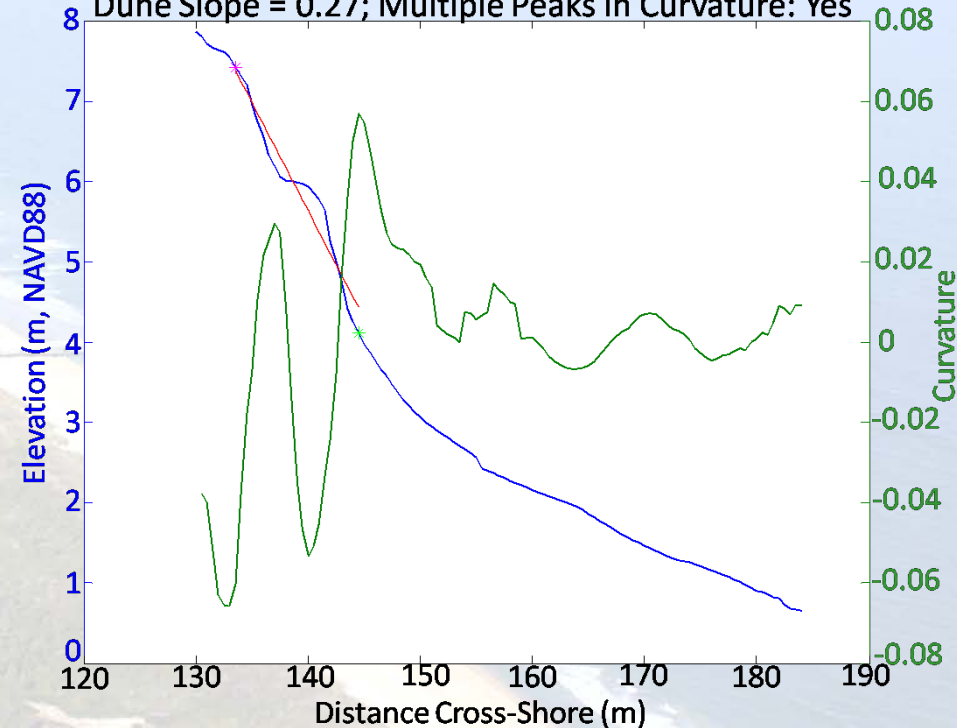Dune Slope = 0.49; Multiple Peaks in Curvature: Yes

Healthy/Mature
Profile at 10801m alongshore
Dune Slope = 0.27; Multiple Peaks in Curvature: Yes
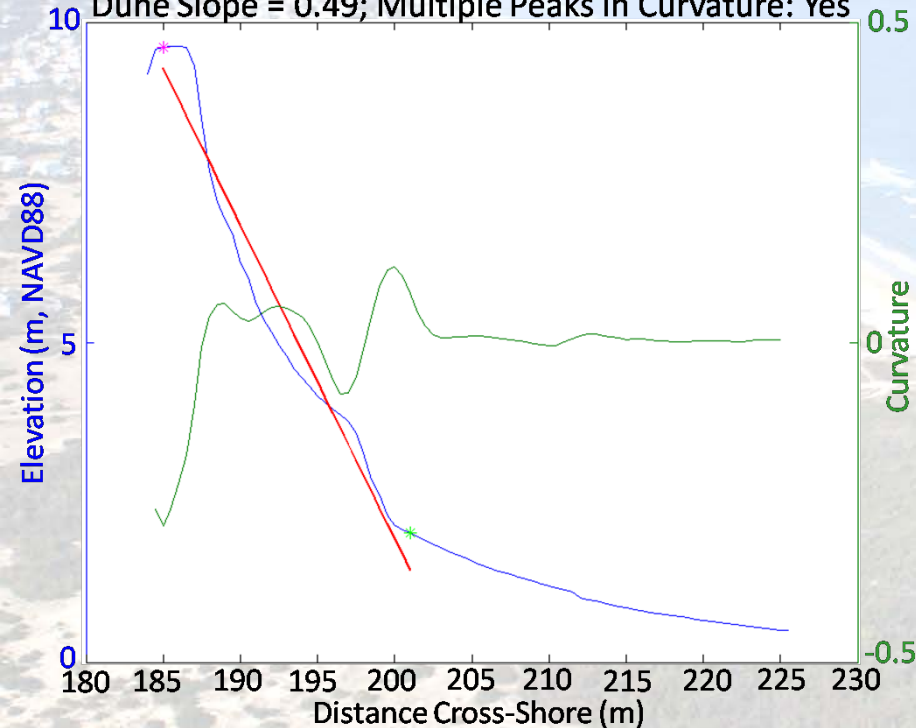
- Incipient dune forms near dune toe (Hesp 2002) while upper dune face remains steep indicating recent wave attack

- Less dune volume compared to healthy dune due to steeper slope on upper dune face

- Continual deposition and re-working by Aeolian processes yields shallower slopes closer to angle of repose for native sediment

- Longer time period since last storm-wave inundation allows for greater dune volumes and prograding foredune face
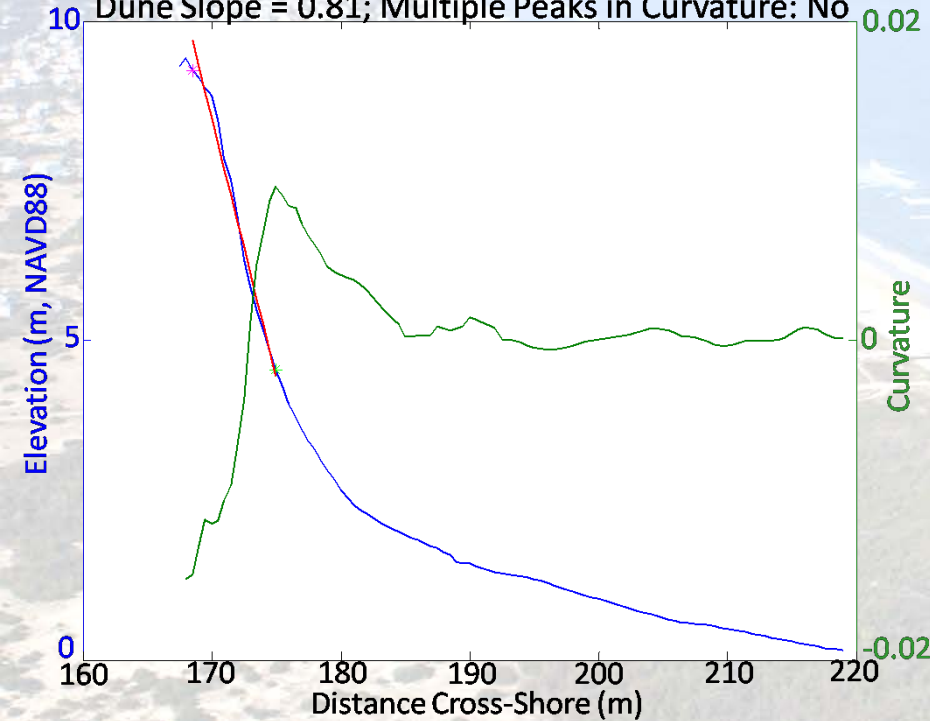
Classification

- Both scarped and man-made dunes are defined by $\kappa_{pks} < 0$ (i.e. NO peaks in curvature)
- Characterized by a more linear foredune face

Scarped
Profile at 16183m alongshore
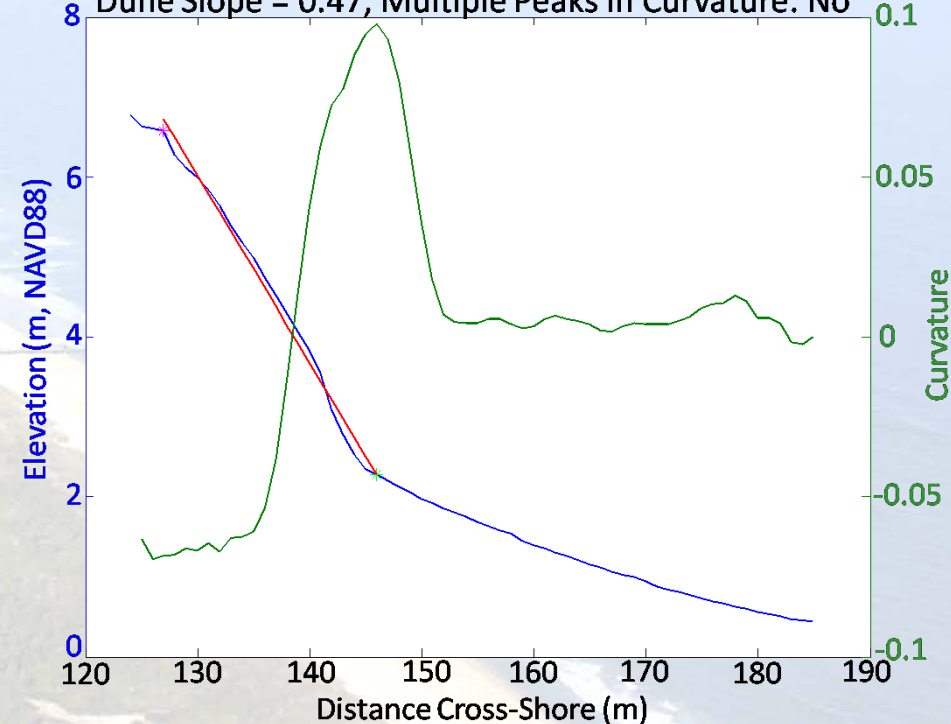Dune Slope = 0.81; Multiple Peaks in Curvature: No

Man-made
Profile at 7546m alongshore
Dune Slope = 0.47; Multiple Peaks in Curvature: No

- Defined by steep slopes and low dune volume, indicative of recent scarping from wave attack

- No incipient dune present and often little to no recovery at the base of the dune

- Larger dune volume and shallower slope approaching angle of repose typically placed as an unconsolidated pile of sediment

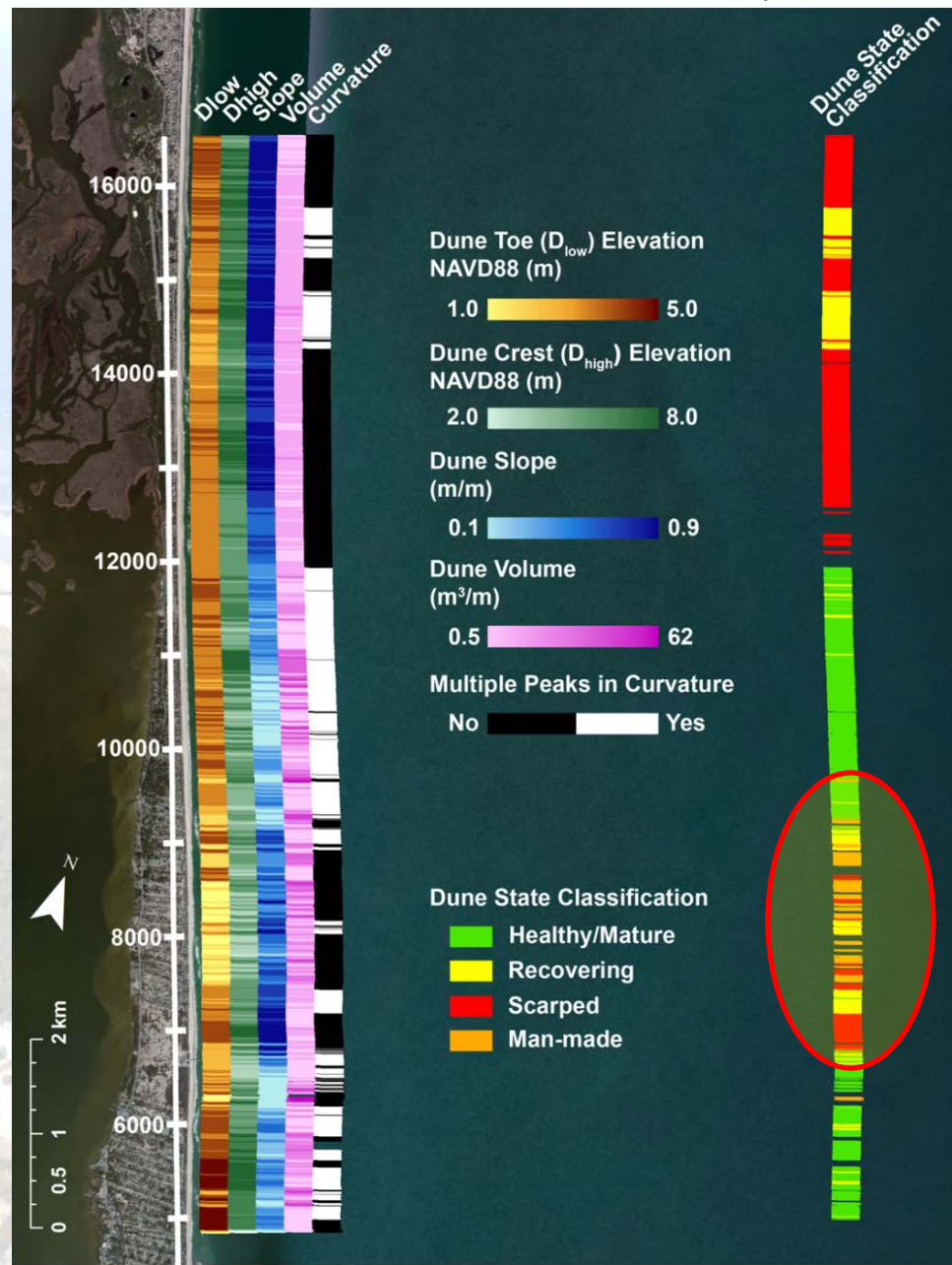- Dune toe elevation often lower due to beach scraping or pushing

Classification - Results

- Final product from classification routine useful for coastal engineers and managers to identify vulnerable areas

- Results were in-line with qualitative assessments of the study site

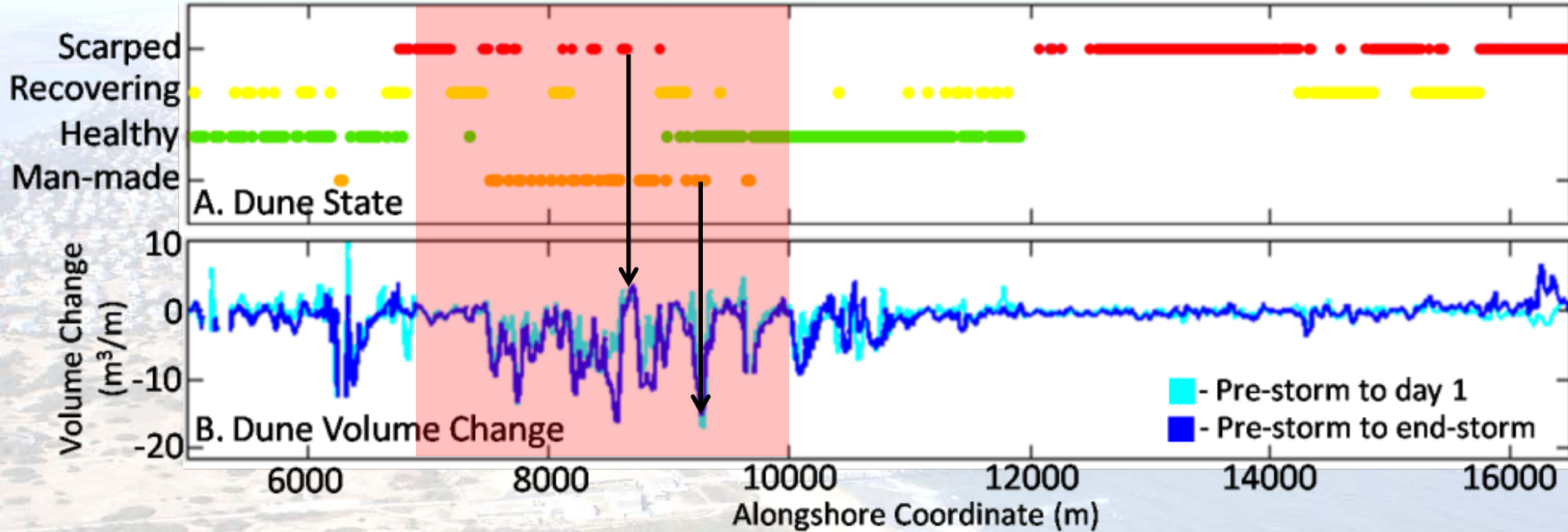- Transitions are still poorly understood and need further investigation

Dlow | Dhigh | Slope | Volume | Curvature

Dune State Classification

Dune Toe (D$_{low}$) Elevation NAVD88 (m)
1.0 — 5.0

Dune Crest (D$_{high}$) Elevation NAVD88 (m)
2.0 — 8.0

Dune Slope (m/m)
0.1 — 0.9

Dune Volume (m³/m)
0.5 — 62

Multiple Peaks in Curvature
No — Yes

Dune State Classification
- Healthy/Mature
- Recovering
- Scarped
- Man-made

Storm Response

A. Dune State

B. Dune Volume Change

- Pre-storm to day 1
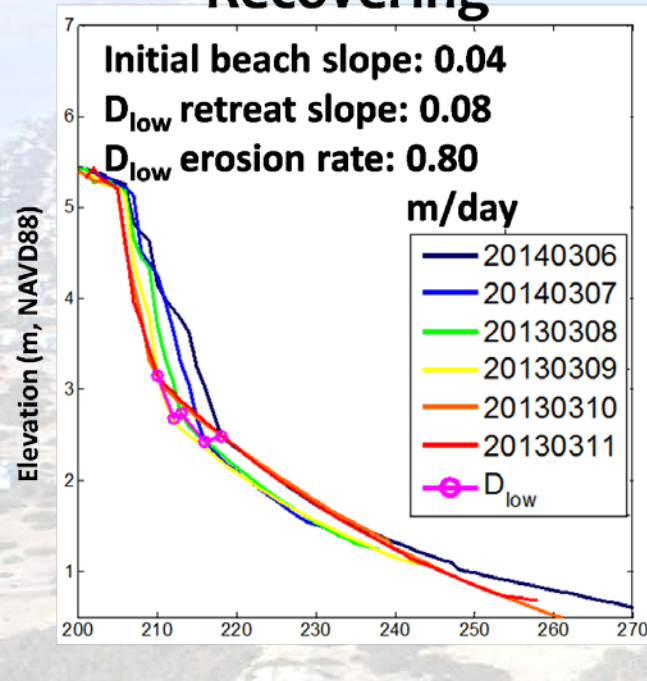- Pre-storm to end-storm

- Dune volume change clearly illustrates where wave attack to the foredune occurred within the study site vs. pre-storm condition

- Highest erosion rates coincide with the erosional hotspot, recently impacted 4 months prior by Hurricane Sandy; particularly the recently constructed man-made dunes
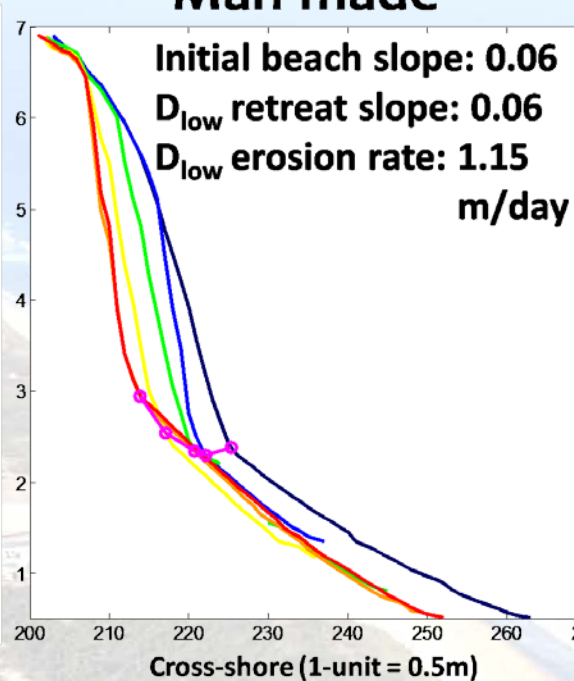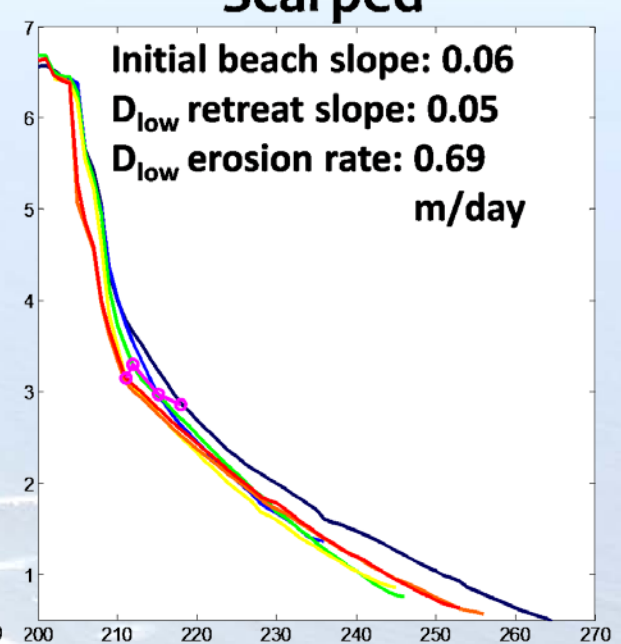
Storm Response

- All three dune types present in erosional hotspot and daily D_{low} erosion rates were calculated

- Recovering and man-made dunes experienced an initial drop in D_{low} elevation whereas scarped dunes retreat was directed upward

- **Hypothesis:** unconsolidated sediment present in both the incipient recovering foredune and the recently placed pile of sand by homeowners combined with lower D_{low} elevations yields higher erosion rates

Conclusions

- Subtle changes in curvature exploited to identify active Aeolian Transport

- Along with foredune slope and volume, useful for indicating "state" of dune

- Classification regime allows for rapid identification of resilient regions and useful for mitigation efforts

- Preliminary storm-response results indicate consolidation affects resiliency and magnitude of retreat

- Classification not necessarily linked to storms → more interested in recovery /resilency
  - Which regions are recovering naturally vs. vulnerable

Future Work

- Classification parameter thresholds calculated using Bayesian Network (Wikle and Berliner 2007)

- Perhaps adapt code for airborne data (JALBTCX, SFM photos)

- Test code in other locations and varying dune types

- Test performance of dune erosion models (Palmsten and Holman 2011) to predict alongshore variations in dune-response using this dataset (consolidated vs. unconsolidated performance)

- More investigation into the transitionary regions and how the hydrodynamics and management practices are different within stretches of coastline that otherwise appear similar

Reference

- Erikson, L. H., Larson M., and Hanson, H.. (2007). "Laboratory Investigation of Beach Scarp and Dune Recession due to Notching and Subsequent Failure." *Marine Geology* 245 (1-4): 1–19. doi:10.1016/j.margeo.2007.04.006.

- Hesp, P. (2002). "Foredunes and Blowouts: Initiation, Geomorphology and Dynamics." *Geomorphology* 48: 245–68. doi:10.1016/S0169-555X(02)00184-8.

- Houser, C. (2013). "Alongshore Variation in the Morphology of Coastal Dunes: Implications for Storm Response." *Geomorphology* 199 (October): 48–61. doi:10.1016/j.geomorph.2012.10.035.

- Larson, M., Erikson, L., and Hanson, H. (2004). "An Analytical Model to Predict Dune Erosion due to Wave Impact." *Coastal Engineering* 51 (8-9): 675–96. doi:10.1016/j.coastaleng.2004.07.003.

- Mitasova, H., Hardin E., and Starek, M.J. (2011). "Landscape Dynamics from LiDAR Data Time Series." http://www.geomorphometry.org/system/files/Mitasova2011geomorphometry.pdf.

- Mitasova, H., Overton M., and Harmon, R. S. (2005). "Geospatial Analysis of a Coastal Sand Dune Field Evolution: Jockey's Ridge, North Carolina." *Geomorphology* 72 (1-4): 204–21. doi:10.1016/j.geomorph.2005.06.001.

- Nordstrom, K. F. (1994). "Beaches and Dunes of Human-Altered Coasts." *Progress in Physical Geography* 18: 497–516. doi:10.1177/030913339401800402.

- Nordstrom, K. F. (2008). *Beach and Dune Restoration*. publisherNameCambridge University Press. http://dx.doi.org/10.1017/CBO9780511535925.

- Nordstrom, K. F., and Jackson N. L. (2013). "Restoration of Coastal Dunes." In , edited by M. Luisa Martínez, Juan B. Gallego-Fernández, and Patrick A. Hesp. Springer Series on Environmental Management. Berlin, Heidelberg: Springer Berlin Heidelberg. doi:10.1007/978-3-642-33445-0.

- Palmsten, M. L., and Holman, R. A. (2011). "Infiltration and Instability in Dune Erosion." *Journal of Geophysical Research* 116 (C10): C10030. doi:10.1029/2011JC007083.

- Palmsten, M. L., and Holman, R.A. (2012). "Laboratory Investigation of Dune Erosion Using Stereo Video." *Coastal Engineering* 60 (February): 123–35. doi:10.1016/j.coastaleng.2011.09.003.

- Sallenger Jr., A. H. (2000). "Storm Impact Scale for Barrier Islands." *Journal of Coastal Research* 16 (3). Coastal Education & Research Foundation, Inc.: 890–95. http://www.jstor.org/stable/4300099.

- Stockdon, H. F., Holman, R. A., Howd, P. A., and Sallenger Jr, A. H. (2006). "Empirical Parameterization of Setup, Swash, and Runup." *Coastal Engineering* 53 (7): 573–88. http://www.sciencedirect.com/science/article/pii/S0378383906000044.

- Stockdon, H. F., Sallenger Jr, A. H., Holman, R. A., and Howd, P. A. (2007). "A Simple Model for the Spatially-Variable Coastal Response to Hurricanes." *Marine Geology* 238 (1–4): 1–20. http://www.sciencedirect.com/science/article/pii/S0025322706003355.

- Thom, B. G., and Hall, W. (1991). "Behaviour of Beach Profiles during Accretion and Erosion Dominated Periods." *Earth Surface Processes and Landforms* 16 (1991): 113–27. http://onlinelibrary.wiley.com/doi/10.1002/esp.3290160203/full.

- USACE, (2013). "Hurricane Sandy Coastal Projects Performance Evaluation Study: Disaster Relief Appropriations Act, 2013." Report submitted to Congress by the Assistant Secretary of the Army for Civil Works, November 6, 2013. http://www.nan.usace.army.mil/About/Hurricane_Sandy/CoastalProjectsPerformanceEvaluationStudy.aspx

- Wikle, C. K., and Berliner, L. M. (2007). "A Bayesian Tutorial for Data Assimilation." *Physica D: Nonlinear Phenomena* 230 (1-2): 1–16. doi:10.1016/j.physd.2006.09.017.

- Woolard, J. W., and Colby, J. D. (2002). "Spatial Characterization, Resolution, and Volumetric Change of Coastal Dunes Using Airborne LIDAR: Cape Hatteras, North Carolina." *Geomorphology* 48 (1-3): 269–87. doi:10.1016/S0169-555X(02)00185-X.

Questions??